

Depth Information from Holographic Radar Scans

C. G. Windsor¹, A. Bulletti², L. Capineri², P. Falorni², S. Valenini², M. Inagaki³,
T. Bechtel⁴, E. Bechtel⁴, A. Zhuravlev⁵, and S. Ivashov⁵

¹116, New Road, East Hagbourne, OX11 9LD, UK

²Dipartimento Elettronica e Telecomunicazioni, Università di Firenze, Firenze, Italy

³Walnut Ltd, 4-2-54 Sakaecho Tachikawa 190, Japan

⁴Enviroscan Inc, 1051 Columbia Avenue, Lancaster, PA 17603, USA

⁵Remote Sensing Laboratory, Bauman Moscow State Technical University, Russia

Abstract— Holographic radar has several potentially important advantages over conventional pulsed radar for buried object location and identification. In particular the sensor can be lightweight, of low cost and provide images of the object with good resolution. This work reports that it can give some depth information also. Two simple experiments using the Rascan system operating at 5 discrete frequencies between 1.5 and 2.0 GHz are described. The first “calibration” experiment used an aluminium plate buried in sand and inclined at a known angle to give a range of depths between 0 and 85 ± 5 mm over a length of 300 mm. The sensor was manually moved on a thin plate of glass placed over the sand above the plate. The scan down the plate showed characteristic bands in the background-corrected reflected intensity — the “zebra effect”. The five reflected amplitudes at each frequency are seen to vary differently with depth. These are interpreted qualitatively in terms of the simple theory involving interference between the reflected wave and the incident wave at the sensor position. This theory does demonstrate the zebra effect and suggests that the amplitude variation with frequency is characteristic of the depth. The cyclic nature of the zebra stripes means that the more frequencies available, the better the depth discrimination. Quantitatively the true theory is complex, especially in the presence of the glass. However we suggest that the measurements can at least be used as calibration signals for a metal reflector at a given depth. The second “test” experiment involved nine US pennies buried in sand at known depths between 0 and 56 mm with a lateral separation of about 50 mm. A background-corrected total reflected intensity (the summed modulus of the reflected amplitude over all frequencies) revealed the outline of each penny quite distinctly. For each penny the set of reflected signal amplitudes at each frequency was determined at the position over the penny where the signal was maximized. This “best” response for each penny gave a response over the five frequencies which was distinctive and is indeed characteristic of the depth. A precise simulation theory is not available but the best frequency response of each penny could be compared with the frequency response curves from the aluminium plate as a function of the known depth. A least squares fit was made between the best amplitudes of as a function of frequency for each penny, compared to the amplitude variation of each frequency as a function of known depth in the inclined aluminium plate experiment. With arbitrary amplitude scaling a least squares residual minimum as a function of depth was always obtained for any one penny. There were some problems. The amplitude scaling varied for each penny, presumably as its surface quality and orientation altered the intensity reflected into the sensor. Also the signal quality deteriorated with depth, and the frequency variation became less distinct at depths greater than 4 cm. However for the six pennies covering the depth range up to 3.4 cm the fitted depth agreed with the actual measured depth to within a standard deviation of 3 mm.

1. INTRODUCTION

Ground penetrating radar has many advantages for the detection of buried objects [1]. However the cost of conventional pulsed systems of order \$200,000 has limited its use particularly in the important area of mine detection. The invention of holographic radar [2] offers similar or better performance for around \$5000 [3]. Holographic radar’s simplicity arises from its use of continuous signals at several different frequencies. The signal is extracted through interference between the wave reflected from the object with the emitted wave. The image of the buried object is built up by moving a scanning head and observing both amplitude and phase changes in the signal. In the Rascan system there are five discrete frequencies between 1.5 and 2.0 GHz and both parallel and perpendicular polarisations [4]. The antenna is moved by hand across the surface to be scanned as shown in Figure 1. The small attached wheel measures the distance along the scan and the operator uses a ruler to determine the scan positions in the perpendicular direction.

The working of the holographic radar system can be expressed most simply by assuming a planar antenna and receiver and a planar reflector at a depth d into the ground. The equation for

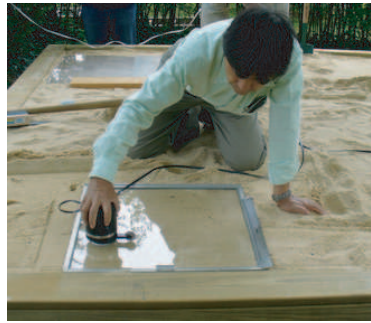


Figure 1: The Rascan system in use on the sand bed at Enviroscan, USA.

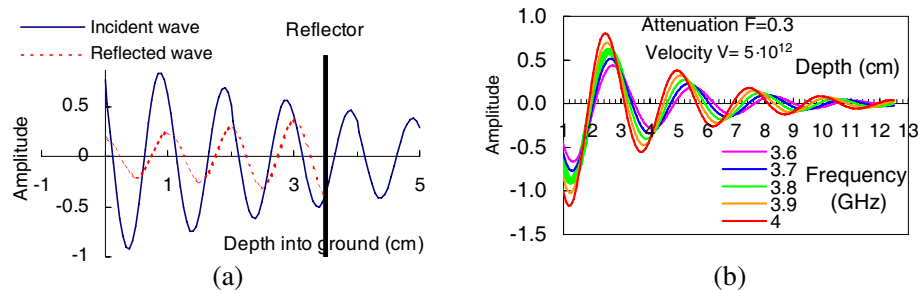


Figure 2: (a) The incident and reflected wave amplitude as a function of depth into the ground with a reflector present at 3.5 cm depth. The phase and amplitude of the two signals are identical at the reflector. (b) The interference signal at the antenna position as a function of the reflector depth as a function of frequency. A velocity of 20 cm, and some frequency dependent exponential attenuation has been assumed.

an incident plane wave travelling along a one-dimensional depth variable x , at time t is $y_{inc}(x) = \cos(2\pi\nu t + 2\pi x/V + \phi_0)$ where ν is the frequency, V is the velocity in the material, and ϕ_0 is a phase factor. The dark continuous line in Figure 2 shows an incident wave of this sort travelling into the ground with some small attenuation factor $\exp(-F(\nu)x)$. The reflected wave from the object at unknown depth d , shown by the dashed line, will travel back in the opposite direction and will have the same phase (or the opposite phase depending on the material) at that spatial position at all times, a different amplitude A , but the same frequency and velocity. Its equation is $y_{ref}(x) = A \cos(2\pi\nu t + 2\pi(d-x)/V + \phi_0)$. When the reflected wave arrives back at the antenna interference holography is performed by effective multiplication of the incident and reflected signals at the position of the antenna. The resulting holographic signal $y_{hol}(0)$ is given by the integration over all phase angles

$$\begin{aligned} y_{hol}(0) &= \int_{0, 2\pi} \cos(2\pi\nu t + \phi_0) A \cos(2\pi\nu t + 4\pi d/V + \phi_0) \exp(-F(\nu)2d) d\phi \\ &= 1/2A \cos(4\pi\nu d/V) \exp(-F(\nu)2d) \end{aligned} \quad (1)$$

and so is sinusoidal with a period depending on frequency, depth and velocity, with an amplitude depending on the position of the reflector as shown in Figure 2(b).

The amplitude is immediately seen to be periodic in depth, with a period $2\nu d/V$ dependent on the frequency. This is the origin of the intensity bands or “zebra effect” seen from sloping objects. It is seen that, at any one depth, the order of the signal as a function of frequency, varies and is to some extent characteristic of the depth. This is particularly true at depths within the first oscillation period. At greater depths, the dependences of amplitude on frequency with depth become similar although remain distinct. It is this distinct variation that offers the opportunity to determine an object’s depth from its variation of reflected amplitude with frequency.

However the simple Equation (1) is not valid in practical situations. In fact the incident wave is created by an antenna of finite shape and distinct geometry. The reflecting object is unlikely to be an infinite plane. There are likely to be other reflecting surfaces, particularly the ground reflections, which cannot be neglected. The ground itself, soil or sand, will introduce its own background scattering. All these effects can in principle be included and a mathematical model of the synthesized microwave hologram for point objects has been presented [4]. At present we have

no such comprehensive model. The method of this paper is to use experimental observations as the model for understanding the reflections from unknown objects.

2. THE INCLINED ALUMINIUM PLATE EXPERIMENT — THE CALIBRATION

A simple sheet of aluminium was used in this experiment to calibrate the holographic signals from an extended metallic reflector as a function of depth. The sheet was about 2 mm thick and 350 mm long and was buried in the sand pit so that it had an inclination of 85 ± 5 mm in 300 mm horizontal distance (15.8°). The top edge of the plate just touched the surface as shown in Figure 3. The Rascan head was scanned along the inclined direction at intervals of 10 mm with the scans separated in the direction perpendicular to the inclination of 10 mm. There were 60 measurements along the direction of inclination and 30 measurements in the perpendicular direction. Measurements were taken in both parallel and perpendicular directions but the results were very similar and only the parallel direction is considered here.

The scan is seen to contain a considerable area of “background”, an “edge” area of complex behaviour which we shall neglect, and an area of “uniform” response from which we can extract as essentially one-dimensional response from the extended plate as a function of depth. A background analysis was first made. This is essential if quantitative amplitudes are to be extracted. A histogram of amplitudes was made over 6 of the scans within the background area and the mean taken for each frequency, and subtracted from the raw amplitude data. 4 scans within the within the uniform area were averaged and a mean amplitude level evaluated for each frequency as a function of the calculated depth.

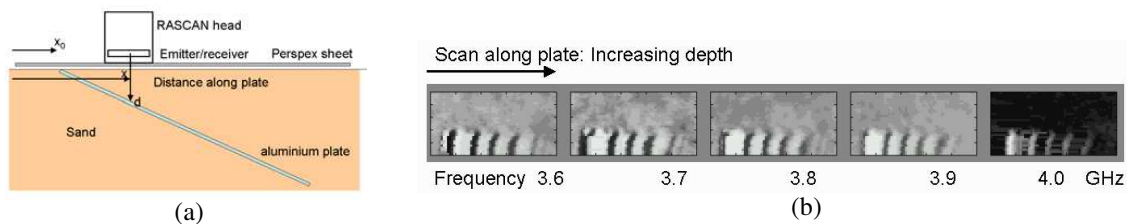


Figure 3: (a) The layout of the inclined aluminium sheet experiment. The Rascan head was manually scanned parallel to the direction of inclination. (b) The grey scale presentation of the holographic data at each frequency presented in the plane of the sheet.

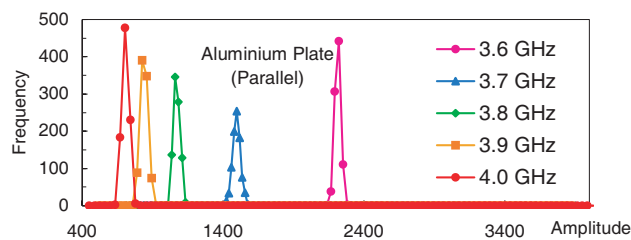


Figure 4: Background determination From six scans in the upper half of the image. The amplitude of each pixel in the image is plotted as a histogram. The centres of the amplitude histogram peak for each frequency is quite distinct.

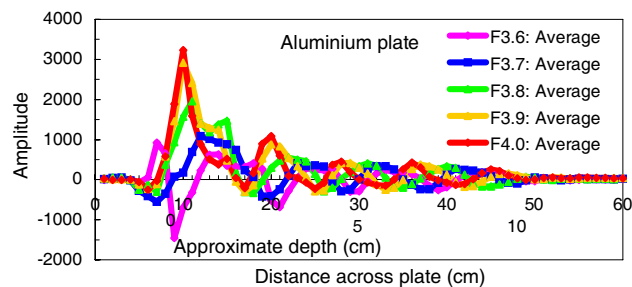


Figure 5: The background-corrected averaged signal from the inclined aluminium plate as a function of distance along the plate for the five distinct frequencies (F) shown.

Having subtracted the mean background level at each frequency, four scans in the lower region of the image showing a strong signal were averaged together for each frequency. The results shown

in Figure 5 show a generally decaying set of amplitudes with the characteristic “zebra” bands of positive and negative amplitude with respect to the background at that frequency. The centres of the bands move characteristically with frequency and this is the key to the depth information.

Figure 5 shows generally a strong similarity to the theoretical description in Figure 2(b). The main difference is around the zero nominal depth position where the experimental curves extend around a centimetre below the nominal zero position. This is not because of the plastic sheet overlaying the sand. In holographic radar the signal from this would be expected to be independent of position and change only the background signal. The most likely causes were mentioned above. The antenna has finite extent and the wavelength of the radar is of order x cm in sand. Both of these cause resolution effects making the measured signal extend beyond the edge of the plate. Of course a similar effect occurs at the deep edge of the plate and the reflected signal is seen to disappear to background levels at around 40 cm lateral displacement.

3. THE BURIED PENNIES EXPERIMENT — THE TEST SITUATION

Nine US pennies were buried in sand at increasing depths from on the surface to 56 mm deep in the same area of sand used in the aluminium plate experiment. Figure 6 shows them as buried, before covering with more sand. The same 60 cm RASCAN was made over the pennies in the direction of increasing depth. Figure 7 shows the resulting images at each frequency.

The scans across the pennies were analysed to find that scan which gave the largest amplitude over each penny. Most of these lay on a single scan, but a few pennies lay off this line and gave a maximum response on other scans. These maximum amplitudes are shown as a function of penny number and frequency in Figure 8. It is a curious graph. The most shallow penny #1 gives only a modest signal with relatively little change of amplitude with frequency. The nominally 10 mm deep penny #2 shows the largest amplitude with a large frequency variation. Pennies #3 to #7 show similar amplitudes but a distinctive frequency variation. Pennies #8 and #9 are distinctly weaker.

These data were analyzed for each penny by least squares fitting the 5 amplitudes from each frequency with the set of amplitudes as a function of depth derived from the aluminium sheet experiment. It was necessary to introduce a arbitrary scaling factor for each penny. Possibly the thickness, reflectivity and specular reflection of the angle of each penny were different leading to a different amplitude factor. However the factor is assumed independent of frequency. Figure 9 shows the actual and fitted amplitudes for the most shallow five pennies. Finally we show in Figure 10 by closed circles the best fitted depths for each penny plotted against the actual measured depths with crosses and error bars. The fit is always within the error bars for the pennies where a good fit was obtained and the standard deviation of the fitted and actual depths is only about 3 mm.



Figure 6: The buried pennies experiment. shows a photograph of the pennies in the sand before being buried. After covering the pennies with more sand their depths were measured by poking with a wooden stick. The radar scans also show a line of metal washers which proved too close together. For accurate analysis, and some foreign Coins of random depths.

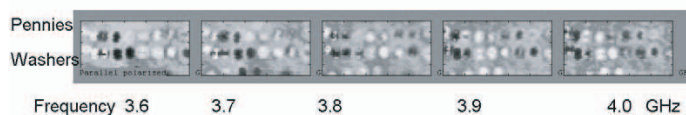


Figure 7: The manual scan of the pennies experiment as a function of increasing penny depth. The variable nature of the phase of the signal is clear. Even the amplitude of the signal appears almost random. While the penny signals appear reasonably separated, this cannot be said of the washers, which have not therefore been analysed.

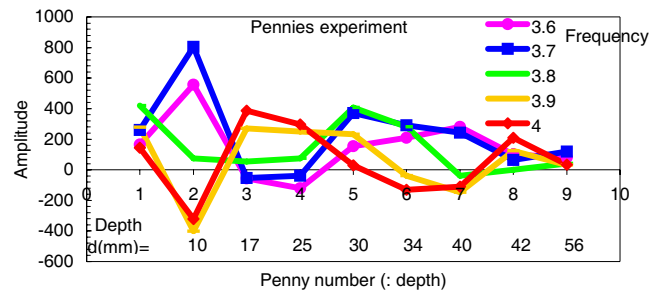


Figure 8: The maximum set of amplitudes seen in any one scan from each penny as a function of frequency.

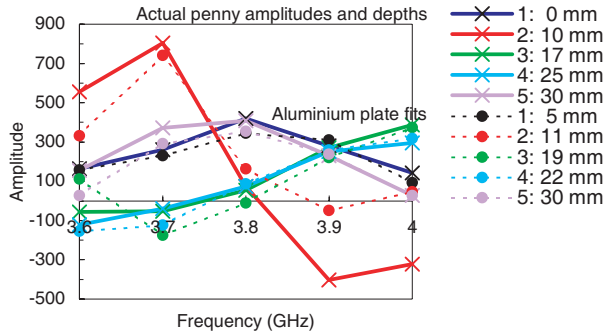


Figure 9: The measured set of amplitudes for each penny (crosses and full lines) fitted to those measured from the aluminium plate experiment as a function of depth (closed circles and dashed lines). The measured depths and the fitted depths are shown. Pennies at greater depths failed to give a good signal.

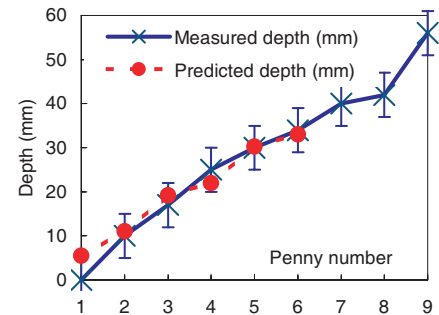


Figure 10: The fitted depths of each penny (closed circles) compared to the a measured depths (crosses with likely errors).

4. CONCLUSIONS

The sloping aluminium plate experiment and the simple theory of beating the incident wave with a reflected wave with phase shift $4\pi\nu/d$ (d = depth) clearly showed the origins and explanation of the stiped “zebra” effect from inclined reflectors.

A good fit to theory is not possible because of the complications of the full probe emitter and object geometry.

The US pennies experiment was analyzed to determine the depths of isolated buried objects. The distinctive frequency response of each penny enabled the depth to be estimated by looking for the same amplitude pattern within the aluminium plate experiment.

The fit to experiment for the first 6 pennies was good to ± 3 mm. More frequencies would lead to a more robust depth algorithm.

REFERENCES

1. GPR Equipment and Service Providers, US Department of Transport pamphlet: <http://www.fhwa.dot.gov/infrastructure/asstmgmt/gprbroc.pdf>.
2. Daniels, D. J., “Surface penetrating radar for industrial and security applications,” *Microwave Journal*, 68–82, December 1994.
3. Chapursky, V. V., S. I. Ivashov, V. V. Razevig, A. P. Sheyko, and I. A. Vasilye, “Microwave hologram reconstruction for the RASCAN type subsurface radar,” *Proceedings of the Ninth International Conference on Ground Penetrating Radar, GPR 2002*, 520–526, Santa Barbara, California, USA, April 29, 2002.
4. Capineri, L., S. Ivashov, T. Bechtel, A. Zhuravlev, P. Falorni, C. Windsor, G. Borgioli, I. Vasiliev, and A. Sheyko, *12th International Conference on Ground Penetrating Radar, GPR 2008*, Birmingham, UK, 2008.
5. Ivashov, S. I., et al., “Holographic subsurface radar technique and it applications,” *12th International Conference on Ground Penetrating Radar, GPR 2008*, Birmingham, UK, 2008.